Sedimentary Geology 294 (2013) 68–82

Contents lists available at SciVerse ScienceDirect

Sedimentary Geology

journal homepage: www.elsevier.com/locate/sedgeo

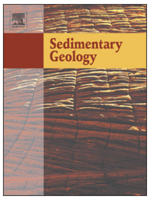

Alternation of microbial mounds and ooid shoals (Middle Jurasssic, Morocco): Response to paleoenvironmental changes

Sara Tomás [a,*], Martin Homann [a,1], Maria Mutti [a], Frédéric Amour [a], Nicolas Christ [b], Adrian Immenhauser [b], Susan M. Agar [c], Lahcen Kabiri [d]

[a] Institute for Earth and Environmental Science, University of Potsdam, Karl Liebknecht-Str. 24-25, Potsdam-Golm 14476, Germany
[b] Institute for Geology, Mineralogy and Geophysics, Ruhr-University Bochum, Universitatsstraße 150, Bochum 44801, Germany
[c] ExxonMobil Upstream Research Company, 3120 Buffalo Speedway, Houston, TX 77098-1806, USA
[d] Faculty of Science and Techniques, University of Errachidia, BP 509, 52000 Boutalamine-Errachidia, Morocco

ARTICLE INFO

Article history:
Received 24 January 2013
Received in revised form 1 May 2013
Accepted 8 May 2013
Available online 25 May 2013

Editor: B. Jones

Keywords:
Microbial mounds
Thrombolites
Ooid shoals
Paleoenvironment
Jurassic

ABSTRACT

The occurrence of neritic microbial carbonates is often related to ecological refuges, where grazers and other competitors are reduced by environmental conditions, or to post-extinction events (e.g. in the Late Devonian, Early Triassic). Here, we present evidence for Middle Jurassic (Bajocian) microbial mounds formed in the normal marine, shallow neritic setting of an inner, ramp system from the High Atlas of Morocco. The microbial mounds are embedded in cross-bedded oolitic facies. Individual mounds show low relief domal geometries (up to 3 m high and 4.5 m across), but occasionally a second generation of mounds exhibits tabular geometries (<1 m high). The domes are circular in plan view and have intact tops, lacking evidence of current influence on mound preferred growth direction or distribution patterns, or truncation. The mound facies consists almost entirely of non-laminated, micritic thrombolites with branching morphologies and fine-grained, clotted and peloidal fabrics. Normal marine biota are present but infrequent. Several lines of evidence document that microbial mound growth alternates with time intervals of active ooid shoal deposition. This notion is of general significance when compared with modern Bahamian microbialites that co-exist with active subaquatic dunes. Furthermore, the lack of detailed studies of Middle Jurassic, normal marine shallow neritic microbial mounds adds a strong motivation for the present study. Specifically, Bajocian mounds formed on a firmground substratum during transgressive phases under condensed sedimentation. Furthermore, a transient increase in nutrient supply in the prevailing mesotrophic setting, as suggested by the heterotrophic-dominated biota, may have controlled microbial mound stages.

1. Introduction

Microbialites (*sensu* Burne and Moore, 1987) have been important contributors to carbonate environments for the last 3.5 billion years (Grotzinger and Knoll, 1999; Hofmann et al., 1999; Allwood et al., 2007; Burns et al., 2009). They encompass a wide range of types of accumulation, including carbonate stromatolites and thrombolites, authigenic accumulations such as some tufa, travertine, speleothem and spring, seep and vein deposits (see Riding, 2011 and references therein for a review) and develop in a wide number of depositional settings (i.e. freshwater, marine, evaporitic, alkaline etc.). After the advent of grazing metazoans in the Paleozoic, many neritic marine microbialite communities withdrew to ecological refuges, where predatory stress is limited (Riding, 2000 and references therein). Previous workers (Grotzinger, 1990; Arp et al., 2001; Riding, 2006) also stressed that secular changes in sea water chemistry may have controlled the long-term distribution of neritic microbial carbonates.

During the Mesozoic, microbialites colonized a variety of neritic marine environments across all latitudes (e.g., Triassic: Riding, 1992; Leinfelder and Schmid, 2000, Late Jurassic: Leinfelder and Schmid, 2000 and early Aptian: Rameil et al., 2010). This widespread distribution pattern is contrasted by the present-day world, characterized by a rather limited occurrence of actively growing stromatolites and thrombolites. Examples include high-energy settings such as Shark Bay, Australia (Logan, 1961; Reid et al., 2003; Jahnert and Collins, 2013) and Eleuthera Bight and Exuma Islands, Bahamas (Dravis, 1983; Dill et al., 1986; Reid et al., 1995, 2000; Andres and Reid, 2006). There, metazoan competition is limited due to non-normal marine environments or high current velocities resulting in constantly moving subaquatic dune substrates that represent significant obstacles for benthic grazers. The Bahamian case examples provide the – at present – perhaps best modern examples of contemporaneously active ooid shoals and microbial carbonate facies. The co-occurrence of these facies types

---

[*] Corresponding author. Tel.: +49 331 977 5851; fax: +49 331 977 5700.
E-mail address: stomas@geo.uni-potsdam.de (S. Tomás).

[1] Present address: Institute of Geological Sciences, Free-University Berlin, Malteserstraße 74-100, 12249 Berlin, Germany.

0037-0738/$ – see front matter © 2013 Elsevier B.V. All rights reserved.
http://dx.doi.org/10.1016/j.sedgeo.2013.05.008

is not without problem as instable substrates (Dravis, 1983; Ginsburg and Planavski, 2008) is often viewed as a critical factor preventing microbialite development. Given the fact that the Jurassic outcrops documented and discussed in this paper refer to combined shoal/microbialite facies in an inner ramp setting, this discussion is of interest here.

Obviously, besides the nature of substratum, a complex suite of environmental characteristics including sedimentation rate (Sun and Wright, 1989; Braga et al., 1995), carbonate saturation state (Fischer, 1965; Grotzinger, 1990; Riding and Liang, 2005), trophic and oxygen levels (Hallock and Schlager, 1986; Leinfelder et al., 1996; McCook, 2001; Camoin et al., 2006), illumination and bathymetry affect microbial carbonate precipitation and result in a bewildering diversity of macro- and microfabrics (Burne and Moore, 1987; Riding, 2000; Reid et al., 2003; Dupraz et al., 2009). This diversity is used as a proxy to infer changes of environmental conditions or biological communities (Harwood and Summer, 2011; Riding, 2011), but different workers seem to disagree in many aspects. With reference to the recent Bahamian examples, stromatolites exhibit laminated and coarse agglutinated fabrics with incorporated detrital, ooid and sand-size components (Dravis, 1983; Dill et al., 1986; Reid et al., 1995; Feldmann and McKenzie, 1998), whereas thrombolites show irregular clotted fabrics with ooids and other detrital particles in unbound-sediment pockets between the mesoclots (Aitken, 1967; Kennard and James, 1986; Feldmann and McKenzie, 1998). This variation might correspond to different benthic communities linked to changes in environments with water-depth (Feldmann and McKenzie, 1998). According to these authors, thrombolites are dominated by algal ecosystems and form in subtidal setting during intervals of sea-level rise, whereas stromatolites consist mainly of cyanobacterial benthic communities and occur in intertidal settings. In contrast, Planavsky and Ginsburg (2009) proposed that clotted thrombolitic fabrics result from the taphonomic remodeling of a precursor (laminated) fabric. Moreover, Riding et al. (1991) describe stromatolites and thrombolites with coarse-grained fabrics growing together in subtidal shoal environments in Miocene deposits of southern Spain and Jahnert and Collins (2013) document the ocurrence of thrombolitic and stromatolitic fabrics in microbial deposits in Shark Bay (Australia) arranged laterally within the same environment.

With respect to the Middle Jurassic world, only few examples of microbially dominated reefal facies (*sensu* Riding, 1991) have been reported (i.e. North Pacific realm: Parcell and Williams, 2005; Ploynoi and Parcell, 2005). Conversely, Middle Jurassic microbialites are often associated with siliceous sponges in deeper water (e.g. Friebe, 1995; Bersán and Aurell, 1997) and with corals in shallower settings (e.g. Olivier et al., 2006; Reolid et al., 2009).

Here, we document and interpret Bajocian shallow-water thrombolitic situated in an inner ramp setting of the Amellago Canyon, High Atlas, Morocco (Figs. 1, 3). Similar to the modern Bahamian case examples, these Bajocian thrombolic mounds are embedded in cross-bedded oolitic facies. In contrast, the Moroccan examples consist of fine-grained clotted peloidal fabrics with scarce or absent detrital particles formed by *in situ* microbially-induced precipitation. Evidence is brought forward, that these two carbonate modes -microbial versus oolite shoals — reflect two temporarily separated, and hence alternating depositional modes.

The aims of this paper are: (i) to document the spatial and temporal relationships between microbial mounds and oolitic shoal facies, (ii) to shed light on the significance of alternating mound and oolite formation in its palaeo-environmental context including relative sea-level change, sedimentation rates, bathymetry, and hydrodynamic level, and (iii) to compare and contrast the Amellago mound case examples with ancient and modern microbial carbonates.

2. Setting

2.1. Regional geology, stratigraphy and sedimentology

The study area is located in the Amellago Canyon, approximately 50 km NW of the city of Rich, on the southern flank of the central High Atlas Mountain range of Morocco. The High Atlas Mountains are an intracontinental fold-thrust belt, formed by the inversion of a pre-existing Mesozoic rift system during the Cenozoic (Jacobshagen et al., 1988; Beauchamp et al., 1996). During the Late Triassic to Early Jurassic, the break-up of Pangea resulted in the opening of the North Atlantic Ocean and development of the ENE-WSW trending High Atlas Rift Basin, connected towards the NE with the western Tethys Ocean (Fig. 1). Ongoing Late Triassic-Jurassic rifting and associated block tilting, caused by normal faults, led to a major marine incursion from the western Tethys and to a hemipelagic depocenter bordered by carbonate platforms (Wilmsen and Neuweiler, 2008).

During the Early Toarcian to Bathonian rift-phase the High Atlas Basin was fragmentated into smaller sub-basins bounded by ridges that represent the crests of the tilted blocks (Brede et al., 1992; Laville et al., 2004). From the Late Toarcian to the Late Bajocian, the depocenters of these sub-basins were filled with hemipelagic marl,

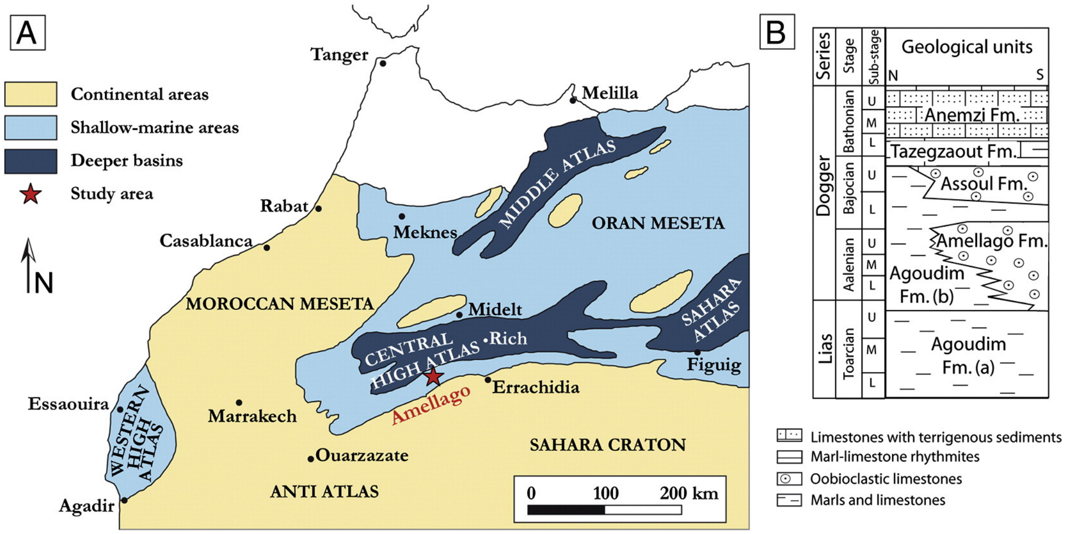

Fig. 1. (A) Map of Morocco showing the main geological units and the position of the village of Amellago in the study area. (B) Regional Middle Jurassic lithostratigraphy of the studied units in the Amellago region (modified after Amour et al., 2012).

while shallow-water carbonate platforms and ramps formed at the margins, one of which is the object of this study.

The study sub-basin shows exceptional exposures of two successive shallow-water carbonate systems (Amellago and Assoul formations) that display similar stacking patterns, facies associations, morphology and size (Amour et al., 2012, 2013). These units include low-angle geometries (0,03 to 0,25° dipping) lacking any margin or high-angle slope and have been interpreted as ramps (Pierre et al., 2010; Christ et al., 2012; Amour et al., 2013). Carbonate deposits consist of cross-bedded, oolitic facies passing basinward into hemipelagic marly sedimentary rocks. The Amellago ramp (Late Toarcian to Early Bajocian) and the Assoul ramp (middle to Late Bajocian) represent two distinct progradational phases onto the basinal marls of the Agoudim Formation (early Bajocian; Fig. 1B).

The Assoul Formation, the focus of this study, consists of 220 m of shallow-water carbonates alternating with subordinate terrigenous sediments (Christ et al., 2012) that deepen towards the NE. The microbial mounds in this study are in the lower part of the Assoul Formation, which represents the initial progradation of shallow-water deposits onto the marls of the Agoudim Formation (Fig. 1B). Recent work by Amour et al. (2012, 2013) differentiated three main depositional environments of the Assoul Formation: inner ramp, mid-ramp and outer ramp (Fig. 2; terminology of Burchette and Wright, 1992).

The innermost ramp depositional environment (paralic facies and tidal flats) is not exposed in the study area. The distal part of the inner ramp, located above the fair-weather wave base (FWWB), includes kilometer-long, peloid-ooid and ooid-dominated sand bodies, which embed microbial-buildups, and marly back-shoal deposits. The fore-shoal, just downdip from the sand bodies, is characterized by rudstone dominated by oncoids.

The mid-ramp, located between the FWWB and the storm weather wave base (SWWB), is composed of mud-dominated lithofacies including gastropods, corals, mollusks, cyanobacteria, and brachiopods at the more proximal part. Toward the distal mid-ramp, oyster-brachiopod-dominated bioconstructions developed in alternation with marly facies (Amour et al., 2012, 2013). The outer ramp comprises the area below

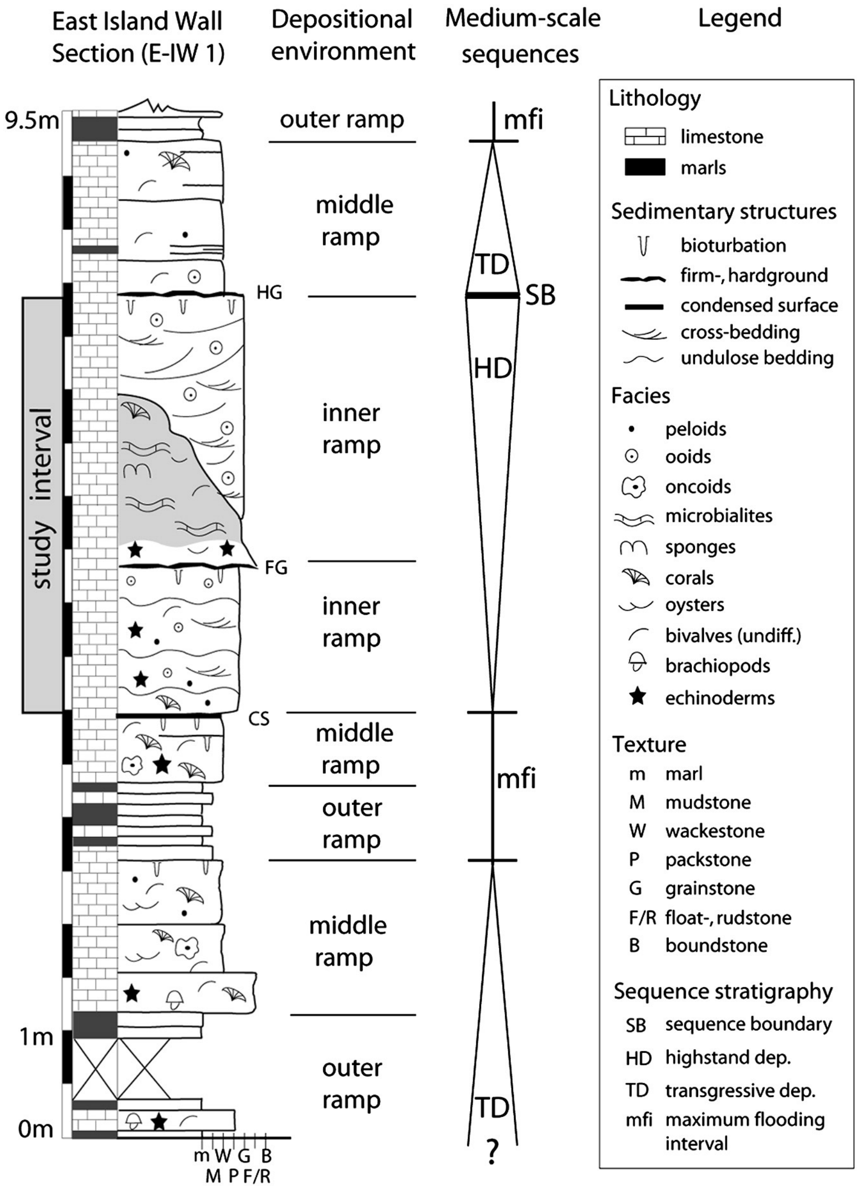

Fig. 2. Stratigraphic section of the East Island Wall outcrop (E-IW1) showing environments of deposition and sequence-stratigraphic interpretation (medium-scale sequences). Transgressive deposits (TD), highstand deposits (HD), maximum flooding intervals (mfi) and sequence boundaries (SB) are indicated. The stratigraphic position of the microbial mounds is marked in grey. CS = condensed surface; FG = firmground; HG = hardground.

the SWWB and is characterized by alternating limestone and marl deposits. The inner to mid-ramp environment includes numerous discontinuity surfaces such as hardgrounds, firmgrounds and condensed surfaces (Christ et al., 2012), interpreted to result from constant wave-action and repeated periods of non-deposition due to slow sedimentation or sediment bypass.

The Assoul microbial mounds seem to be a local feature and pass laterally into well-bedded oolitic packstones and grainstones towards the southeastern and eastern portions of the ramp system. Towards the south and west of the study area, the mound interval is not exposed; towards the north, inaccessible cliffs limits an investigation of what might be the mound interval (Fig. 3A). Two different outcrops of the Amellago Canyon, referred to as “East Island Wall” (E-IW) and “North Island Face” (N-IF) (Fig. 3A) facilitated tracing the characteristics of the microbial mounds spatially. The East Island Wall is located at the eastern side of an erosional remnant here referred to as the “Island”, which is surrounded by the Gheris River on three sides (Fig. 3A). The Island is 310 m long and 190 m wide and is separated northeastwards by the river from the cliff wall of the North Island Face. The Assoul mound interval is exposed over a length of 70 m in the eastern Wall (E-IW) and of 80 m in the northern Face (N-IF) (Figs. 3A, 6A) and is correlated easily between these two outcrops.

2.2. Sequence stratigraphy

Previous sequence-stratigraphic analyses in the lower part of the Assoul shallow-water carbonates of the Amellago area (Amour et al., 2012, 2013; Christ et al., 2012) provide a framework for this study. These authors identify five subtidal medium-scale sequences (~20 m-thick) bounded by regionally extensive hardgrounds. Each medium-scale sequence is composed of small-scale sequences of ~1 to 5 m-thickness delimited by discontinuity surfaces. The terminology of depositional sequences applied here follows the time-independent definiton of Strasser et al. (1999).

The mound interval forms part of the medium-scale sequence that marks the initial progradation of Assoul Formation onto the basinal marls of Agoudim Formation (Fig. 2; medium-scale sequence 1 in Fig. 4 of Amour et al., 2013). This initial sequence is composed of a lower, deepening-upward interval or transgressive deposits (TD), a maximum-flooding interval (mfi), followed by an upper shallowing-upward interval or highstand deposits (HD) (Fig. 2). Transgressive deposits consist of packstone-marl alternations and skeletal wackestones (locally floatstones) with open-marine biota. The maximum-flooding interval is represented by alternate mudstone-marls and wackestone beds, and is capped by a surface of condensation. The highstand deposits include grain-supported lithofacies (oolitic deposits) and associated microbial buildups (Fig. 2).

3. Field approaches and analytical methods

A total of 28 mounds were identified; 14 in each outcrop face. Stratigraphic surfaces, height, width, horizontal spacing and orientation of the mounds were measured using a differential global positioning system (LEICA d-GPS 1200) and a laser locator. A detailed stratigraphic section logged in the Eastern Island Wall outcrop (Fig. 2) illustrates the vertical and lateral variability of the microbial mounds and associated facies, with focus on texture and composition.

Three well-preserved mound structures were sampled systematically and are described in detail here. A total of 52 rock samples were collected from these three mounds and the associated facies. A total of 40 thin sections were studied with a petrographic microscope (LEICA DM RXP). In addition, 47 polished slabs were used to study macroscopic features.

For scanning electron microscopy (SEM) and energy-dispersive X-ray spectroscopy (EDX) analysis, seven rock chips were selected based on their microbial content and state of preservation. The chips were polished and the surfaces were cleaned in distilled water and dried for 10 minutes. Afterwards, the chips were etched in 2% hydrochloric acid for 1 min, rinsed in distilled water and immediately dried and carbon-coated. To avoid contamination, samples were kept isolated in a sterile desiccator. The samples were analyzed on a JEOL JSM - 6510 SEM operating at 11–15 kV and equipped with an Oxford

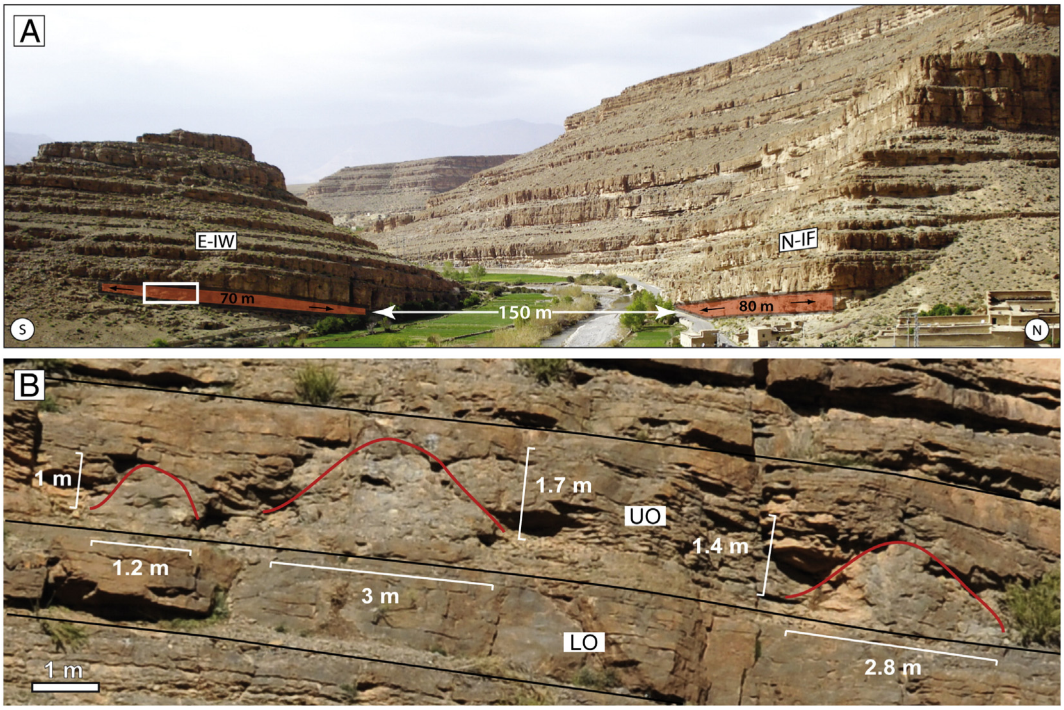

Fig. 3. (A) Panoramic view of East Island Wall (E-IW) and North Island Face (N-IF) in the Amellago Canyon. Microbial mound interval and its exposed lateral extent are marked by red overlay. (B) Close-up image (for location see white box in A) showing the domal morphologies and dimensions of microbial mounds. Note that the mounds occur surrounded by cross-bedded ooid facies. LO = lower ooid unit; UO = upper ooid unit.

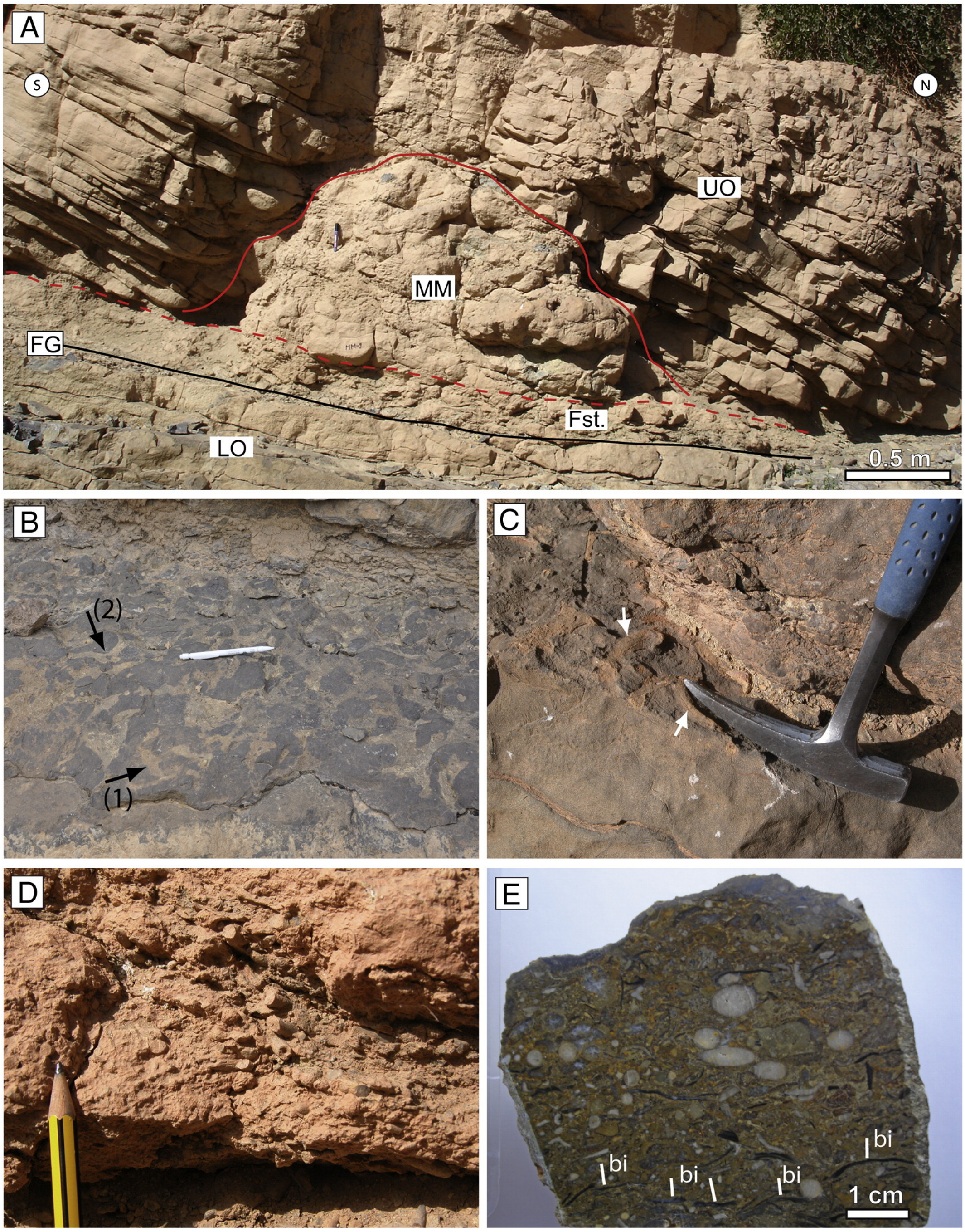

Fig. 4. (A) Outcrop view of a microbial mound and associated facies. The microbial mound (MM) overlies a firmground (FG) at the top of the lower ooid unit (LO). The mound grew on top of an echinoid and oyster floatstone layer (Fst.). The upper ooid unit (UO) surrounds and overlies the mounds, and drapes the mound morphology. Note cross-beds with high-angle (25°) foresets and dominant northward dip direction. (B) Outcrop view of the firmground (FG) showing different stages of lithification. (1) Burrow with irregular walls pointing to unlithified substratum and (2) Burrow with sharp borders pointing to bioturbation of partially lithified substratum. (C) Close-up view of the firmground (FG) showing horizontal burrows with sharp contacts to the host carbonate rock (arrows). (D) Close-up view of the thin layer of floatstone at the base of the mounds that includes abundant echinoid spines. (E) Polished slab of the echinoid-oyster floatstone lithofacies showing disarticulated, horizontally oriented bivalve shells (bi).

Instruments EDX system. The elemental composition and mappings obtained with the EDX were analyzed with the Microanalysis Suite INCA 4.15 from Oxford Instruments.

4. Description of mounds and associated facies

The microbial mounds are distributed within a discrete interval (~4 m thick) and are easily recognized throughout the whole succession due to their characteristic weathering morphology and lack of internal bedding (Fig. 3B). The mounds form elevated structures, surrounded by planar and trough cross-bedded deposits (Fig. 4A).

The deposits underlying the mounds consist of ooid packstone and grainstone with undulose bedding and low-angle planar cross-bedding (lower ooid unit). Ooids commonly are micritized and small (~0.4 mm). The ooids show internal fabrics with few fine radial laminae (type 4 defined by Strasser, 1986) and less abundant coarse radial cortices (type 5 of Strasser, 1986), suggestive of intermittent high energy and relatively low energy, respectively (Strasser, 1986). Peloids (0.2 to 0.5 mm) and various bioclasts (coral, echinoid and bivalve debris) also are common in these units. A marker interval with abundant horizontal burrows and accumulations of brachiopod shells caps the lower unit (FG in Figs. 2, 4B). This interval can be traced laterally over distances of hundreds of meters throughout the Island section. Individual burrows display a sharp contact with the encasing sediment (Fig. 4C). The stratigraphic contact between the marker interval and the overlying mounds is sharp but lacks evidence for erosion. No lithified clasts or components such as ooids from the lower unit were found in thin sections from the mounds.

The base of the mound is a laterally continuous, 40-cm thick echinoid-oyster floatstone that passes upward into the microbialite fabric (Fig. 4D). The echinoid plates and oyster shells are disarticulated and oriented horizontally (Fig. 4E). Other minor components are brachiopods, bryozoans, gastropods, and coral fragments. The mounds pass laterally and upward into ooid grainstone, locally packstone (upper ooid unit). The ooid beds show high-angle planar cross-bedding and occasionally trough cross-bedding with foresets showing a marked dominant dip direction (up to 25°) towards the north (Fig. 4A). They include asymmetric and symmetric oscillation ripples and rare bidirectional ripples. The ooids are in average twice as large (~0.8 mm) as those in the lower unit, and are less micritized. The ooids of this unit are dominantly types 4 and 5, as those in the lower unit, but ooids with fine radial cortices (type 3) also are present. The latter suggests high water energy during deposition (Strasser, 1986). Scarce peloids and skeletal fragments occur within this upper oolitic unit.

Commonly, the ooid unit drapes the mounds, and oolitic facies downlap onto the mound flanks (Fig. 4A). The contacts between the mounds and oolitic beds are sharp and well-defined (Fig. 5B). However, in places the flanks of some mounds are laterally adjacent with the ooid beds without showing a clear temporal order (Fig. 5A), and a oolitic bed (Fig. 5C) lies above an apparent truncation surface in at least one mound (UO in Fig. 5C).

Locally, a second generation of mounds occurs above the first one, separated by ooid beds of the upper ooid unit. These mounds exhibit tabular morphologies (~80 cm high) with marked lateral accretion (Fig. 5D) and are overlian by the upper oolite. In places, this second mound generation does not occur or it may amalgamate with the deposits of the first mound phase (Fig. 5A).

4.1. Dimensions, morphology and growth patterns of the mounds

The Bajocian mounds in the Amellago Canyon are isolated structures and exhibit meter-scale elevated domal morphologies. The horizontal spacing between single mounds is variable and ranges from 1 to 6.5 m. The height of individual mounds ranges between 0.5 and 3.2 meters and their apparent width is between 1.2 and 4.7 meters (Fig. 3B). The mounds have a generally consistent height/width ratio close to 0.5, independent of the mound dimensions. No marked differences or any changing trend in mound heights are evident between the two outcrops. The field observations did not allow for a direct observation of the true three-dimensional mound morphology but the measurement data show that the cross-sectional width of the mounds does not change with changes in orientation (Fig. 6), so they are likely circular forms.

Generally, the tops of the mounds are intact and rounded, not truncated or flat (Fig. 5A and D). In instances in which two mounds develop close to one other (~1 to 1.5 m), they coalesce laterally, and form bridge-like connections (Fig. 7A). The underside of these

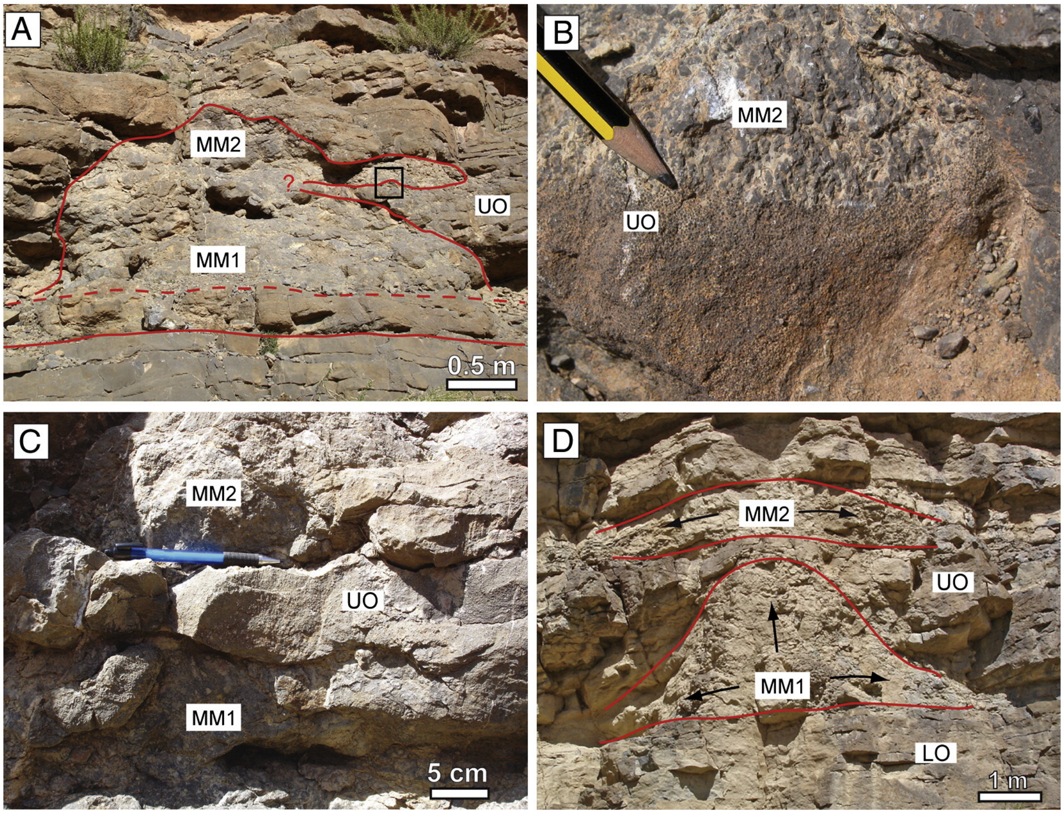

Fig. 5. Outcrop photographs of the microbial mound and surrounding ooid facies. (A) Mound laterally adjacent with, and apparently interfingering with, the upper ooid unit. The lower mound appears to have accreted vertically, forming an elevated structure (MM1). On top of MM1, a second mound generation (MM2) appears to grow preferentially laterally (upper right part). Ooid deposits (UO) only partially overlie the first mound, leading to amalgamation of the two mounds generation. (B) Close-up outcrop view showing sharp stratigraphic contact between a second mound generation (above) and the upper oolite (below) fabrics. For location see box in (A). (C) Ooid bed (UO) separating two beds of microbial mound facies. The ooid unit truncates the first mound generation (MM1) and underlies the second mound generation (MM2). (D) Mound (MM1) with domal morphology buried underneath the upper ooid unit. Subsequent to burial, a second mound with tabular morphology and marked lateral accretion developed (MM2). LO = lower ooid unit; UO = upper ooid unit.

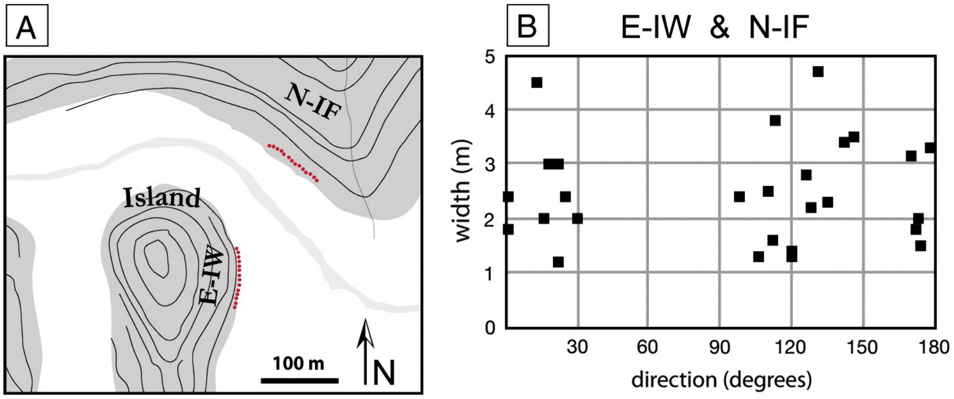

Fig. 6. Map showing location and orientation of all studied mounds (red dots) in the East Island Wall (E-IW) and North Island Face (N-IF) outcrops. B) Plot of cross-sectional widths versus orientation for all studied mounds in both outcrops (E-IW and N-IF). The absence of correlation between these two parameters suggests no elongation along a preferred direction.

connections is composed of "nodular downfacing hemispheroids" (Leinfelder et al., 1993), of approximately 30 cm in thickness, which reflect downward growth of the mound into the subtrate (Fig. 7A and B).

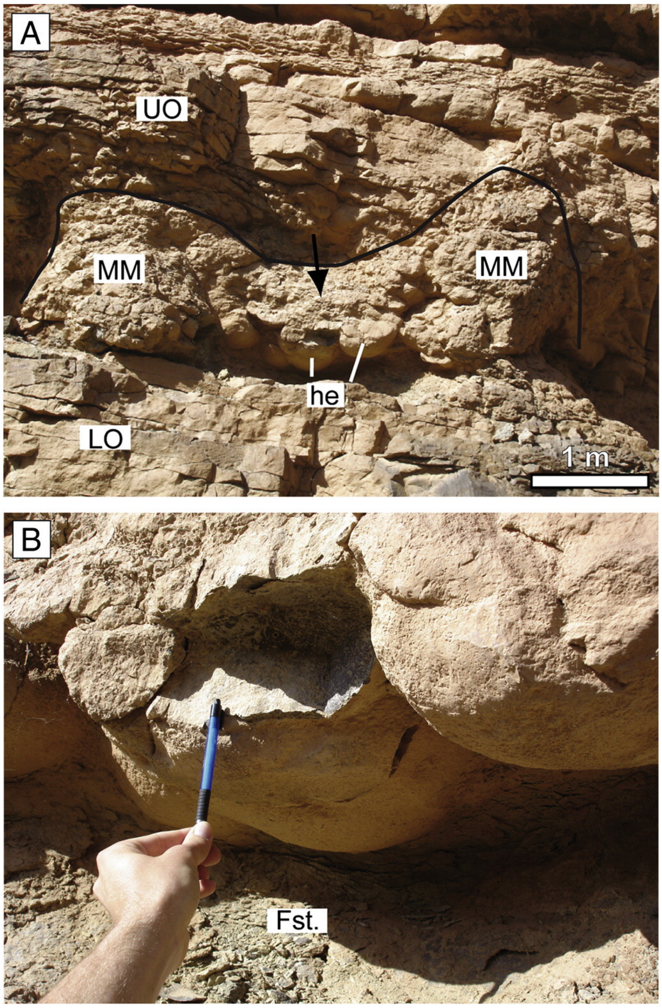

Fig. 7. (A) Two laterally connected mounds (MM) forming a bridge-like structure (bridge) with hemispheroids (he) growing on the lower surface. (B) Close-up view of the hemispheroids. Note downward facing growth into the substrate. LO = lower ooid unit; UO = upper ooid unit; Fst = echinoid and oyster floatstone layer.

4.2. Mound fabrics and composition

The mound framework is comprised almost exclusively (~90%) of microbialites (Fig. 8A), with a subordinate faunal assemblage and few large (up to several centimeters) cavities that collectively constitute up to 10% of the overall mound framework (Fig. 8B). The cavities are distributed regularly and infilled by internal sediment, which is typically non-clotted micrite (commonly recrystallized or dolomitized) or microsparite; rarely, undifferentiated bioclasts occur in these cavities. The faunal elements, consisting mainly of corals, sponges, bryozoans, bivalves and echinoids in growth position, are scattered throughout the microbial mound (Fig. 8B).

Few scattered calcite pseudomorphs after gypsum also occur in the thrombolitic fabric. Energy-dispersive X-ray spectroscopy analysis shows that only minor sulfur inclusions (30 μm in size) are still present inside the crystals. The gypsum pseudomorphs show displacive forms and occur as single lenticular crystals or as aggregates (rosettes). They have dimensions of 4 mm in length and 1 mm in width (Fig. 9A and B). The pseudomorphs occur sparsely in the cavities of the thrombolites and locally, in encasing oolite wackestone to packstone facies (Fig. 9A and B), particularly in the areas in close contact with the thrombolites.

4.3. Microbial fabric

The microbialites mainly exhibit a thrombolitic fabric, recognized by its clotted structure with no internal lamination (Aitken, 1967), composed of mesoclots and mm-scale cavities. Internally, the thrombolites show fine-grained (micritic, peloidal) microfabrics (Riding, 2008). The mesoclots, mesostructural components of the thrombolite (*sensu* Shapiro, 2000), are up to a few millimeters in size and display an arborescent morphology (Fig. 8A and C). Each mesoclot consists of homogeneous dense micrite and peloids that range from 30 to 60 μm across. Although some peloids show well-defined edges, most are densely packed with diffuse edges. The micrite and peloids can form aggregates which are surrounded and traversed by fenestral microspar matrix resulting in the widespread "clotted" fabric ('grumeleuse' fabric of Cayeux, 1935) (Fig. 8D). Allochthonous fine-sand particles, including undifferentiated microfossils in the thrombolite fabric, are rare to absent. Scattered calcite pseudomorphs after gypsum and pyrite crystals are present. Mesoclots agglutinate into 0.5 to 2 mm-wide interconnecting branches, resulting in a complex framework. The thrombolite branch in a slightly digitate fashion, radiating outwards and upwards (Fig. 8C), except in the hemispheroids, where they show downward direction of enlongation (Fig. 8A). Some mesoclots show irregular and diffuse internal layering visible by the difference in light-dark intensity of the layers, which is generated by variations in the micrite/peloid packing density (Fig. 8C).

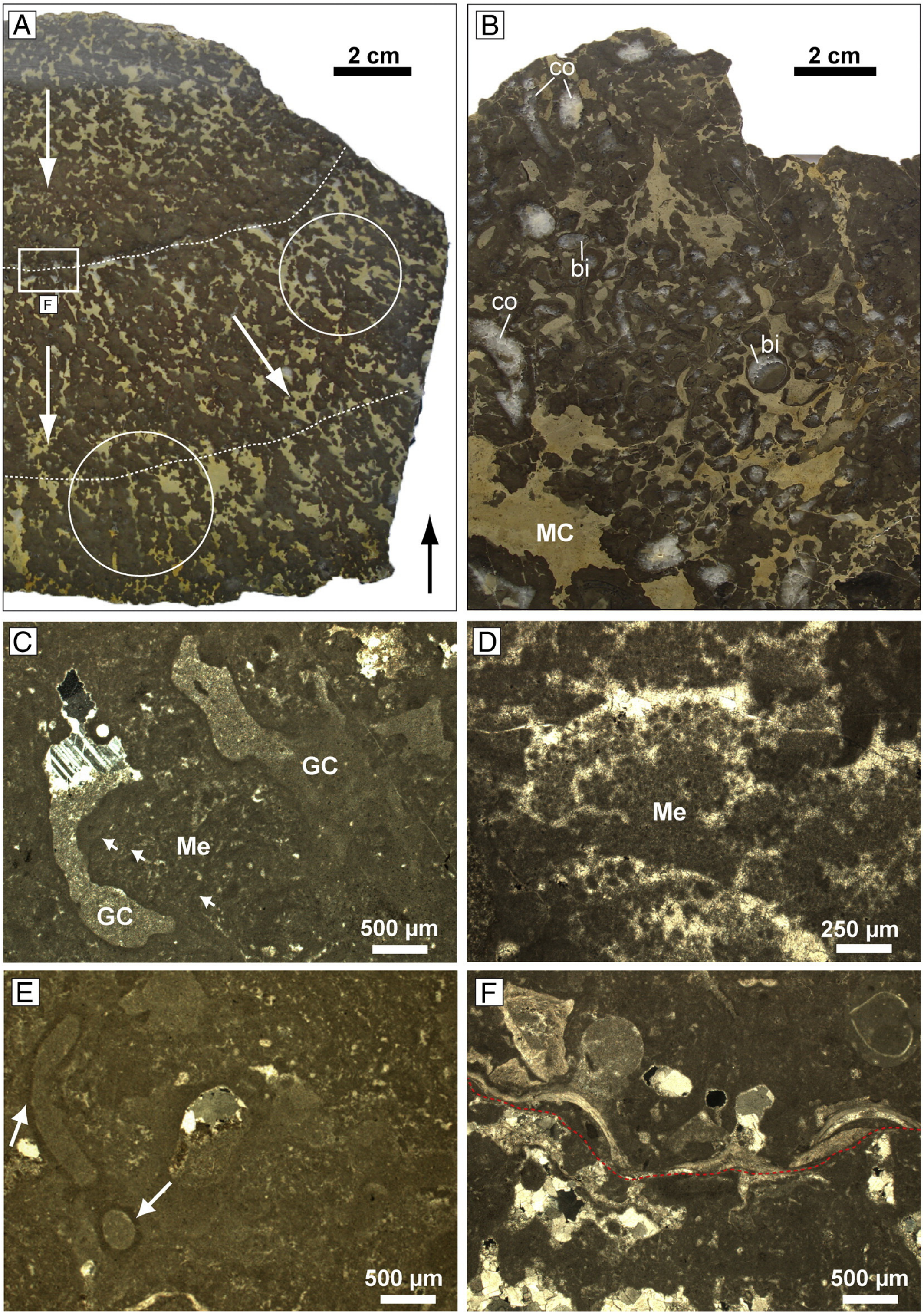

Fig. 8. Polished slab and thin-section photographs of microbial mound fabric. (A) Thrombolite hemispheroid with clotted mesostructure (micritic dark mesoclots) and growth framework cavities filled with micrite and sparry calcite. Stratigraphic up is indicated by the black arrow. The thrombolites show branching forms (circles) radiating outwards and downwards (white arrows). Note regularly distributed intervals of encrustation and bioerosion (dashed lines). (B) Microbial mound framework thrombolites with associated branching corals (co), bivalves (bi) and irregularly distributed large cavities filled with micrite (MC). (C) Detail of thrombolite fabric with micritic mesoclots (Me) composing branches and defining growth framework cavities (GC). Note diffuse internal layering (arrows) and upward accretion of the thrombolite branch. (D) Detail of the mesoclot microfabric composed of micrite and peloids surrounded by microspar (fenestrae). Note that dark micrite and well-defined individual peloids grade into clotted peloids. (E) Burrows within thrombolite interpreted to have formed in semi-consolidated material. Note the dark densely amalgamated material forming the burrow margins (arrow) that grade into adjacent thrombolite fabric. (F) Close-up view of encrustation and bioerosion by bivalve and annelids at outermost surface of the thrombolite (dashed line). For location see box in A.

Irregular cavities occur in the spaces remaining between mesoclots (Fig. 8C, D and E). Cavities are a few mm to 1–2 cm in length and width, and are infilled with micrite or sparry calcite, or both, with geopetal features (Fig. 8E). Cavities are arranged radially, following the branching growth morphology of the thrombolites, and commonly are connected to one another to form a complex three-dimensional network.

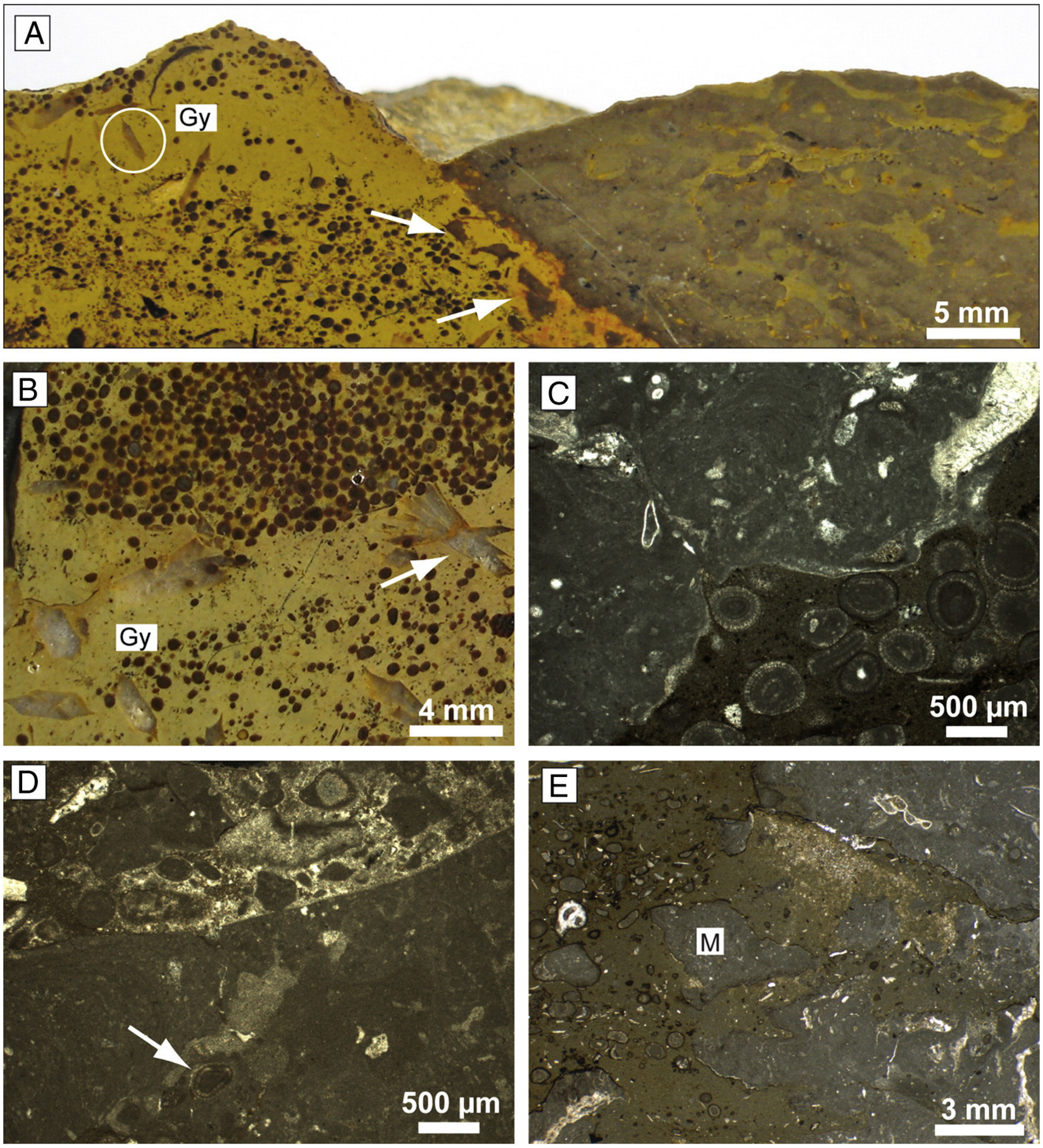

Fig. 9. Polished slab and thin-section photographs of contact area between thrombolite and the adjacent ooid facies. (A) Thrombolitic clotted fabric (right) is clearly distinguished from the ooid packstone (left). Microbialite clasts locally occur within the grainy lithologies (arrows). Note presence of calcite pseudomorphs after gypsum with lenticular morphologies (Gy) inside ooid packstones (circles). (B) Close-up view of gypsum pseudomorphs (Gy) showing displacive morhologies, lenticular and rosette-like crystal aggregates (arrow) inside the ooid packstone. (C) Close-up view showing sharp contact between the thrombolite (upper left) and younger ooid packstone (lower right). (D) Ooid (arrow) enclosed inside a thrombolite growth framework cavity. (E) Close-up view of microbial clasts (M) which have been eroded and incorporated in the oolitic deposits.

In thin section, the micrite infilling the cavities differs from the dense and clotted micrite forming the thrombolites in that it includes less packed and non-clotted fabric, with common recrystallization. The contact between the thrombolite buildups and the adjacent or overlying oolitic facies is sharp (Fig. 9A, C and D). In rare instances, ooids and small bioclasts are evident within the cavities of the thrombolite, particularly in those located near the contact with the encasing oolitic unit (Fig. 9D). Locally, reworked thrombolite clumps are incorporated within the ooid facies (Fig. 9A and E).

4.4. Macro- and microfaunal assemblages

The mounds were inhabited by corals, sponges, bryozoans, bivalves, echinoids, and green algae (*Thaumatoporella*). Annelids and bivalves are the main bioeroders. The organisms are scattered randomly within the thrombolitic fabric and no evidences of growth interruptions in the microbialite are observed, beside some heavily encrusted and bioperforated horizons with high concentrations of bivalves. Thus, it is suggested that the aforementioned organisms colonized the mounds when they were still alive and active. Corals are relatively scarce and mostly occur in life position. Most corals exhibit branching morphologies, although some platy forms are present. Coral skeletons are strongly recrystallized, making their identification difficult (Fig. 8B). Sponges consist mainly of calcareous forms (Order *Pharetronida*), and some siliceous demosponges (lithistids) and spicules also occur. Bryozoans are abundant and mainly represented by the cyclostomate form *Berenicea*. They commonly encrust corals, bivalves or thrombolite mesoclots and in the upper part show erected branches. The green alga *Thaumatoporella* is rare and, where present, encrusts the surfaces of the thrombolite mesoclots in association with bryozoans.

The surfaces of the mounds are wavy and traversed by sinuous, spar-filled burrows. The margins of the burrows are sharp and dark and show compressed and partly amalgamated micrite/peloids (Fig. 8E). Additionally, episodes of pervasive encrustation and bioperforation by bivalves and annelids are abundant above some mound surfaces (Fig. 8F); bivalve bioperforations also cut some of these surfaces. The surfaces are distributed more or less regularly in the mounds and are visible particularly in the hemispheroids, where they have spacing of approximately 5 to 10 cm (Fig. 8A).

4.5. Mineral and biogenic structure

Scanning electron microscope (SEM) observations of the thrombolite fabric reveal that it consists of a honeycomb-like pattern formed by a meshwork of subpolygonal to subspherical pits (3-10 μm in diameter) and walls (1–2 μm thick) (Fig. 10A and B). Spherical bodies are embedded within this meshwork. The spheres are 1 to 3 μm in diameter and commonly appear adhered to one other, to form aggregates (Fig. 10D). Energy-dispersive X-ray spectroscopy analysis show that both the spheres and honeycomb-like meshwork (Fig. 10D and A) are composed of calcium carbonate with high admixture of silicates (Al – K – Fe – Mg). Within the honeycomb pattern, precipitates of high-Mg calcite form small aggregates (1–2 μm) that merge to large, rounded aggregates (5–10 μm) (Fig. 10E).

Small, dark-red spheroidal and cubic mineral aggregates (5 to 15 μm in size) appear scattered throughout the thrombolite fabric. Scanning electron microscope observations of these aggregates reveal that they commonly are encased by calcite and consist of randomly distributed, euhedral (octahedral) microcrystals of pyrite of 0.5 to 2 μm in length, which commonly occur in clusters of four or more specimens (Fig. 10F). They are interpreted as pyrite framboids.

5. Interpretation and discussion

5.1. Fabric origins

The internal structure of Amellago Canyon mounds typically consist of thrombolites with branching morphology (Fig. 8A) and irregularly clotted microfabrics that lack lamination (Aitken, 1967). The clotted appearance is produced by micritic patches and silt-size peloids within a fenestral microspar matrix (Fig. 8C and D). The irregular internal cavities within the thrombolites are interpreted to have formed during deposition, as indicated by their regular spatial distribution and radial orientation, following the space left in between the branching mesoclots and due to the fact they do not truncate the mesoclots (Fig. 8A and C). Therefore, they are here referred to as growth framework cavities (GC) (Pratt, 1995), to emphasize that they formed during the thrombolite growth.

Clotted and peloidal microfabrics, as those in Amellago, are attributed to carbonate precipitation linked to microbial processes, as they constitute the most common microfabric of modern and ancient microbialites (Monty, 1976; Kennard and James, 1986; Dupraz and Strasser, 1999; Riding, 2000, 2008; Dupraz et al., 2009), although Cayeux (1935) considered clotted fabric to result either from partial re-crystallization or mechanical deposition of peloids. The descriptive term “peloid” refers to granular micritic aggregates of uncertain origin (McKee and Gutschick, 1969). They can include allochthonous grains with various origins (Macintyre, 1985). Peloidal fabrics have been regarded as microbial or as cement fabrics (Macintyre, 1985), although these designations are not mutually exclusive (Riding and Tomás, 2006, and references therein). Chafetz (1986) suggested that peloids can be calcified bacterial aggregates. This view is supported by association of $CaCO_3$ precipitation with heterotrophic bacteria in modern mats (Paerl et al., 2001), and by peloidal aggregates resembling bacterial microcolonies constituting the microfabric of calcified biofilm (Riding, 2002). Riding and Tomás (2006) reported that clotted and peloidal fabrics in microbial carbonates possibly result from calcification just below the sediment-water interface in microbial mats, a view echoed by subsequent workers (Spadafora et al., 2010). The former authors suggested that the peloids and the inter-peloid space were created concurrently by bacterial degradation of organic matter, as indicated by a regular organization of the clotted fabrics with typically silt-size peloids and even-spaced peloidal masses, and that the inter-peloid voids (fenestrae) were protected from infiltration of extraneous sediment by the organic-rich exterior surface of the microbialite. Similarly, Pedley (2013) has observed that precipitation in freshwater microbial biofilms occurs in the form of amorphous calcium carbonate nanosphere clusters (micro-peloids) that are focused in specific intra-EPS sites (i.e. close vicinity of living filament and coccoid bacterial clusters), producing thrombolitic carbonate fabrics. The preservation of open fenestrae within the thrombolitic fabrics is related to the loss of the EPS link to the living biofilm surface and to the sealing effect of the living biofilm cover. The fine-grained clotted peloidal microfabrics of the Amellago mounds show relatively regular organization of the peloidal masses and scarcity of incorporated grains, particularly in the inter-peloid voids supporting a microbial origin.

The honeycomb-like patterns within the studied thrombolites, similar to those observed in modern and fossil microbialites, are interpreted to be the result of selective degradation and mineralization of extracellular polymeric substances (EPS) (Défarge et al., 1996; Kazmierczak et al., 1996, 2009; Dupraz et al., 2004). Moreover, the size (1-3 μm), and composition (calcium carbonate with admixtures of Al-K-Fe-Mg silicates) of the spherical bodies embedded within the honeycomb meshwork of the thrombolites resemble mineralized remains of coccoid bacteria in modern microbial mats (Kazmierczak et al., 1996, 2009; Byrne et al., 2001). The rounded aggregates of high-magnesium calcite observed in the honeycomb structures of the Amellago thrombolites can be interpeted as the centers of nucleation for the peloids akin to those structures reported by previous authors (Dupraz et al., 2004; Aloisi et al., 2006).

Beside the *in situ* microbially-induced calcification, allochthonous grain trapping and binding are the most important processes for the growth of modern microbialites in Shark Bay and the Bahamas (Kempe et al., 1991; Riding, 2000; Planavsky and Ginsburg, 2009; Jahnert and Collins, 2013), whereas it appears to be insignificant in the Amellago thrombolites. The Amellago thrombolites comprise pervasive fine-grained micritic (dense, clotted, peloidal) fabrics with scarce or absent allochthonous fine sand-size particles, suggesting they are almost exclusively autochthonous. Similarly, this observation is interpreted for most of the Neoproterozoic-early Phanerozoic thrombolites (Planavsky and Ginsburg, 2009). Nevertheless, the possibility that some carbonate mud particles were trapped in the Amellago thrombolites cannot be completely discounted since it is very difficult to distinguish between trapped carbonate mud and microbially-induced mud. In sum, based on the observations of i) regular and pervasive clotted and peloidal fabrics (Fig. 8C and D), ii) scarcity of incorporated grains from the adjacent sediment (i.e. fine-sand particles, ooids) within the thrombolites, and iii) presence of honeycomb structures and spherical bodies that resemble bacterial remnants (Fig. 10A–E), Amellago mounds can be interpreted as thrombolites, and that their clotted fabrics formed *in situ* by very early diagenetic processes driven by bacteria.

The presence of burrows at the surfaces of the thrombolite bodies indicates their early lithification, favoring their preservation potential. However, compressed and partly amalgamated micrite and peloids marginal to burrows (Fig. 8E) suggest only partial lithification of the accreting thrombolite (Riding and Tomás, 2006). The occurrence of surfaces with pervasive bivalve encrustation and bioerosion distributed regularly within the microbialites may reflect changes in the environmental conditions, such as increase in the nutrient content, akin to those suggested by Dupraz and Strasser (1999).

The small volume of calcite pseudomorphs after gypsum, their extent limited to within and near the mounds and their displacive lenticular and rosette-like crystal morphology suggest that the gypsum formed within micritic mud during early diagenesis, likely from SO_4-enriched fluids that were generated within the mounds through microbial activity and then filtered out.

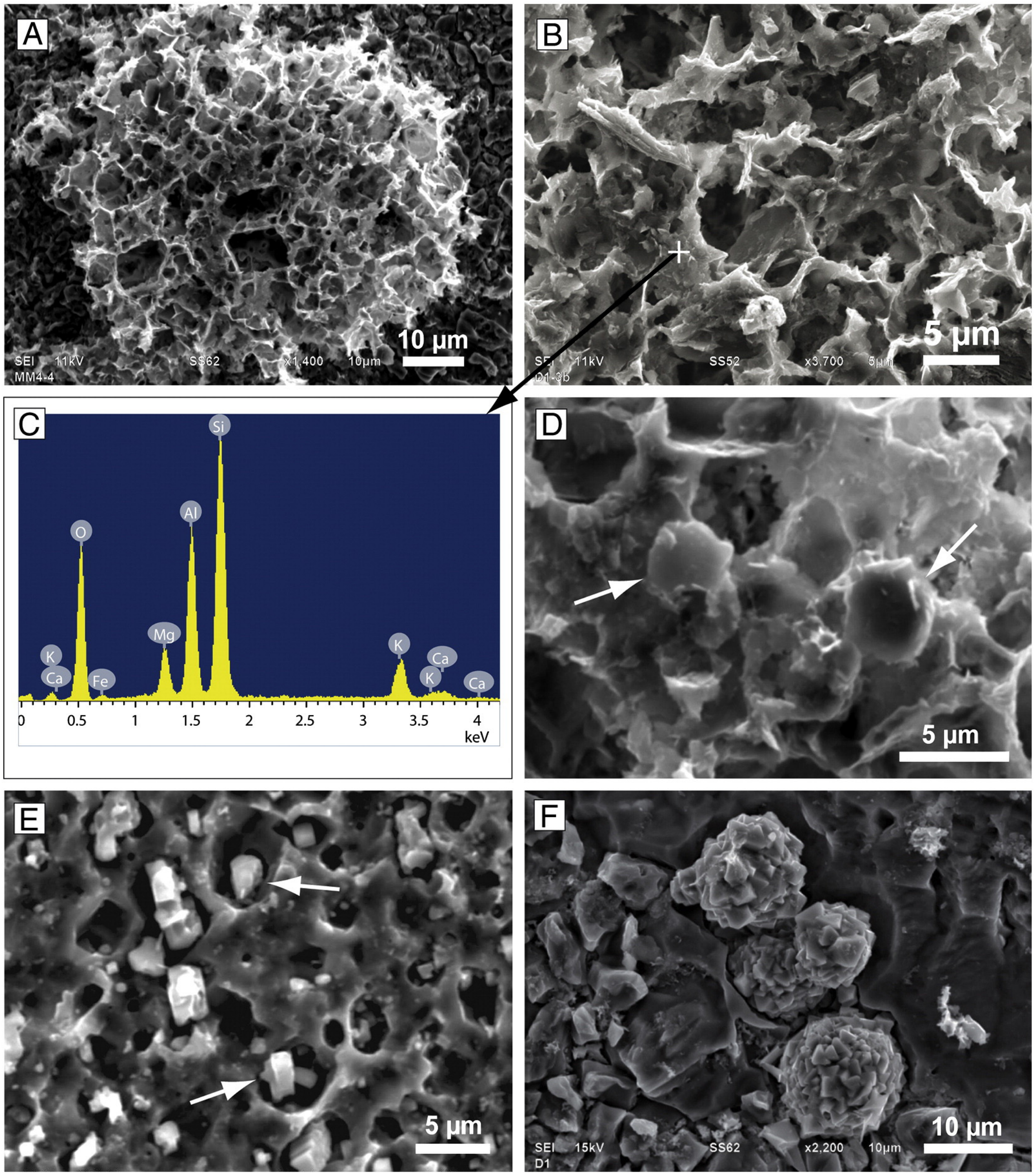

Fig. 10. Scanning electron microscopy photomicrographs of interpreted preserved microbial- and mineral structures. (A) Honeycomb-like pattern of subpolygonal to subspherical pits and walls interpreted as calcified extracellular polymeric substance (EPS) matrix. (B) Close-up view of the honeycomb-like EPS matrix showing pits and walls. (C) EDX spectra showing the elemental composition of the meshwork (white cross in B). The main components are calcite with high admixtures of Al, Fe silicates and some Mg and K. (D) Spherical bodies (arrows) interpreted as coccoid bacteria embedded within the interpreted EPS. (E) Precipitates of high-Mg calcite (arrows) that nucleate inside the pits of the EPS and fuse to form larger aggregates. (F) Framboidal aggregates of pyrite composed of closely packed microcrystals and encased by calcite. cts = counts per second. keV = kiloelectron volt.

5.2. Relationships between microbial mounds and oolite shoals

The inner domain of the ramp of Assoul Formation include oolitic units with exposed dimensions of several kilometers (Fig. 3) that surround the microbial mounds. The oolite passes into peloid-ooid deposits towards the distal parts of the inner ramp. These deposits have been interpreted collectively to represent active shoals. The occurrence of symmetrical and asymmetrical ripples and cross-beddings in the shoals indicates that the bars formed and moved by unidirectional and bidirectional currents, probably by waves and tides (Amour et al., 2013).

There is no evidence for estimating absolute paleo-depth in the Assoul ramp. However, calculated paleo-depth suggested for the different settings of the Amellago ramp (Pierre et al., 2010, Table 1) are considered good analogues for the Assoul ramp due to the similar facies distribution, morphology and dimensions of both ramp systems (Amour et al., 2012). Pierre et al. (2010) have estimated that the subtidal inner ramp is located within 0 to 3 m water depth.

Judging from these outcrops, the overall geological setting, and the stratigraphic relationships between the Amellago microbial mounds and associated shoals, the mounds probably were a spatially localized features of the inner ramp, around or below FWWB. The biota inhabiting the mounds (bivalves, bryozoans, brachiopods, corals, sponges, and green algae) and the lack of subaerial exposure features indicate that the mounds formed under normal marine, subtidal conditions. The light-dependent biota (corals and green algae *Thaumatoporella*) in the mound fabric are evidence for an overall shallow-marine, photic environment. The change in mound growth, from mainly vertical (first mound generation) into mainly lateral (second mound generation), may suggests a decrease in accommodation space that defines the maximum potential growth height of the microbial structure. This view is supported by Andres and Reid (2006), who examined the growth morphologies of extant marine stromatolites from back reef lagoonal settings in Exumas, Bahamas, and relate them to available accommodation space, and linked sedimentation and hydrodynamics. These authors suggest that lateral growth is primarily the result of limited accommodation space, which implies shallow environments with higher wave action.

The sharp contacts between the oolite and mound facies, the common downlapping relations between oolite and mounds indicate that the ooid sand migrated after the mound development. Locally, however, the shoals did not completely cover the first mound phase, and the second mound phase grew upon the first. This amalgamation leds to a single, large mound structure (Fig. 5A). The rare occurrence of ooids into some of the open mound cavities near the contact with the oolites suggests the infiltration of ooids into these cavities during transitional phases between mound and ooid shoal stages when both carbonate facies might have co-occurred for limited time intervals.

In the case of modern Bahamian microbialites, under the influence of currents reaching velocities of up to 150 cm/s (Dill, 1991), the microbialites are characterized by grainy fabrics. Some Bahamian stromatolites are dusted and buried with ooid sand during each tidal cycle and incorporate sand-size detrital particles (Dill et al., 1986; Reid et al., 1995; Feldmann and McKenzie, 1998; Planavsky and Ginsburg, 2009). By comparison, some ancient microbialites with coarse fabrics have been considered good analogs of these modern examples (e.g., Miocene stromatolites and thrombolites from Spain, Riding et al., 1991; Aptian thrombolites from Oman, Immenhauser et al., 2005; Rameil et al., 2010). The absence of allochthonous coarse sediment within the fine-grained micritic mound fabrics of Amellago suggests a different genesis, in an overall low-energy environment as currents would have mobilized ooids from nearby shoals and these would have been incorporated in the mounds. Stromatolites and thrombolites growing in high-energy ooidal channels, as documented in the Exumas, in fact commonly alternate microbial fabrics with redeposited ooid sand layers or sand-size detrital particles (e.g. Feldmann and McKenzie, 1998; Planavsky and Ginsburg, 2009).

Furthermore, modern Bahamian microbialites form columns or ridges elongated and streamlined by tidal currents (Dill et al., 1986; Reid et al., 1995; Feldmann and McKenzie, 1998; Planavsky and Ginsburg, 2009). Immenhauser et al. (2005) documented a preferred orientation of the long axis of Lower Aptian ellipsoidal microbial-foraminiferal buildups, interpreted to reflect hydrodynamic control. In contrast, the overall circular to sub-circular shape of the Amellago mounds (Fig. 6) indicates lack of current influence on the mound distribution pattern in plan view. The observation that mound tops are rounded, intact, and not truncated or flattened indicates that they did not reach the wave base, as interpreted for the flat, table-like examples from the Early Aptian of Oman (Immenhauser et al., 2005). Therefore, the low energy conditions that characterize the mound stages in Amellago differ substantially from the higher-energy regime active during ooid shoal stages. Although the tops of the mounds are not truncated, the occurrence of some intraclasts of thrombolite facies in the oolitic deposits may indicate some local, slight erosion of older mound buildups during the migration of high-energy shoals.

5.3. Change in environment and relative changes in sea level

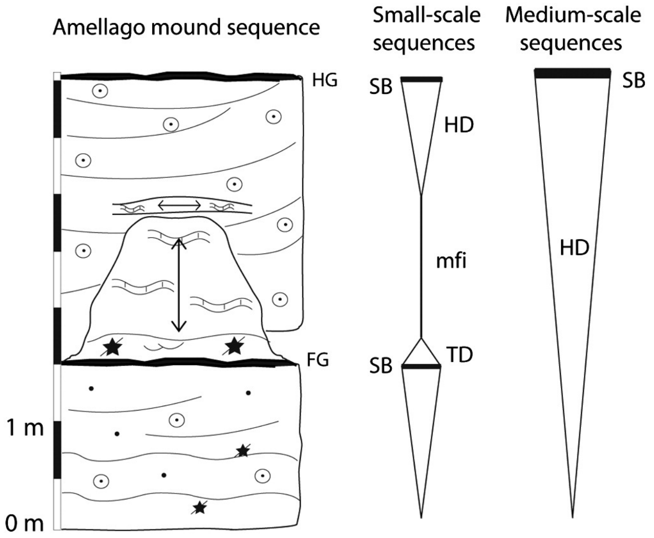

Fig. 11. Sequence stratigraphy interpretation for deposition of the Amellago mound succession. The model shows the medium-scale sequence and internal small-scale sequences interpreted in the mound interval. See Fig. 2 for description of the lithofacies and environments of deposition. Transgressive deposits (TD), highstand deposits (HD), maximum flooding intervals (mfi) and sequence boundaries (SB) are indicated. FG = firmground; HG = hardground. The arrows indicate the preferential, vertical vs. lateral, growth of the mounds.

The microbial mound interval occurs in the highstand deposits (HD) of a medium-scale sequence composed of several small-scale sequences (Figs. 2, 11). A conceptual sedimentologic and environmental model explaining the alternation of mound development and ooid sand deposition suggests changes in water energy in shallow subtidal areas of the inner ramp. These changes, that control the deposition of the small-scale sequences, may be governed by relative sea level variations of high-frequency and low amplitude. The small-scale sequences are indicated by the rhythmic deepening- and shallowing-upward trends of lithofacies throughout the 100 m thick stratigraphic interval of Assoul Formation (Amour et al., 2013). The interval displays repetitive staking pattern of facies bounded by firm- to hardgrounds (Christ et al., 2012). Each of these depositional packages is similar in thickness (few meters) and shows a deepening-upward trend that is sometimes missing, and a clear shallowing-upward trend. These small-scale sequences stack into coherent trends forming the medium-scale sequences (Amour et al., 2013). Nevertheless, the significance of local environmental changes on the transport and deposition of lithofacies was proposed by Amour et al. (2013) on the basis of the mosaic-like distribution pattern of the shoal facies (Burgess, 2008).

The microbial mounds flourished under open-marine, subtidal conditions and represent the transgressive deposits of a small-scale sequence (Fig. 11). The underlying deposits correspond to a firmground with accumulations of shell fragments and burrows with sharp contact with the host carbonate facies. This firmground is interpreted as the sequence boundary of the small-scale sequence and is suggested to be the result of slow accummulation rates, possibly related to a sea-level fall, a decrease in accommodation space and winnowing of sediment on the seafloor in the zone of permanent fair-weather wave action (Christ et al., 2012). Subsequently, sea-level rise resulted in the deposition of a thin (40 cm) bed of echinoid and oyster floatstone at the base of the mounds, here interpreted as a transgressive lag deposit. The disarticulated and horizontally oriented echinoid plates and bivalve shells (Fig. 4E) indicate some amount of transport at the onset of the transgression (Fig. 11). Alternatively, echinoids and bivalves may have colonized inactive areas of the shoals. Nevertheless, the scarcity of ooids or lithoclasts incorporated into this bed and the evidence for some transport is not consistent with the notion of stabilized shoal flanks.

Microbial (thrombolitic) mounds are interpreted to have formed during combined conditions of overall transgression, low energy (fine-grained fabrics) and low sediment rate (condensation). Transgressive stages, creating new accommodation space and pushing the carbonate factory landwards may lead to a transient halt or at least reduction in carbonate production (sediment starvation) expressed in the numerous condensed surfaces, firmgrouds and hardgrounds present throughout the Assoul Formation (Christ et al., 2012). The transgressive phases may also increase the supply of nutrients, which in a mesotrophic setting would shift temporarily the carbonate production to more nutrient-rich (more mesotrophic to eutrophic). It is well known that in modern reef environments, waters characterized by high nutrient concentrations favor blooms of benthic microbial communities (Hallock and Schlager, 1986; McCook, 2001; Mutti and Hallock, 2003; Camoin et al., 2006). Although firm evidence for the recognition of nutrient concentration in the Mesozoic is difficult to establish, in the Amellago ramp the heterotrophic-dominated biota associations (i.e. oysters, brachiopods, echinoids) may reflect moderate nutrient contents (mesotrophic). Nevertheless, there is no direct information concerning the source of the nutrients. These nutrient enriched conditions, combined with the reduced detrital sediment input during transgression, would have benefited microbialite growth, because microbial communities are not able to survive high sediment input (Sun and Wright, 1989; Dromart, 1992; Keupp et al., 1993). In other time-equivalent settings (i.e. Late Jurassic), increased of nutrients linked to transgressions have resulted in oxygen depletion (Leinfelder, 1993; Leinfelder et al., 1996) and promote microbialite growth. Additionally, in the Amellago examples a firmground forming the sequence boundary provided a hard and stable substrate, a critical factor required for the establishment of the microbial communities (Dravis, 1983; Ginsburg and Planavski, 2008). The vertical accretion of the mounds indicates unlimited accommodation space. Occasionally, a second generation of mounds, which acreted laterally (Fig. 11), may develop above the first one, if accommodation space is reduced. Subsequently, during the highstand, the ooid shoals could deposit and prograde over the mounds.

The occurrence of the thrombolite mounds is only specific to the lowest part of the Assoul Formation, which correspond to the onset of a transgression. This occurrence suggests that a number of factors (i.e. high-frequency changes in water energy and depth), favoring the mound development find the ideal conditions just at this initial transgressive stage, when the sea level rise at a significant pace and there is a pronounced increase in the accommodation space at the same time that the sediment production is low. As discussed above further high-frequency paleoenvironmental fluctuations, such as a threshold in the range of water depth and an increase in nutrient availability that bring the system into more nutrient-rich conditions, must be reached to guarantee the growth of the microbial mounds.

Subsequently, once the system became shallower (above wave base) and more agitated, ooid shoal deposition took over. Obviously, during the transitional phase between mound and ooid shoal stages, shoal and mound formation might have coexisted in time. The abrupt change from grainy (oolites) to muddy (mounds) facies and the local and short-lived distribution of the microbial mounds along the section suggest that microbial growth reflects combined conditions of low energy, low sedimentation rates, increased water depth and nutrients.

6. Comparison of Amellago Canyon mounds with coeval microbialites

To the knowledge of the authors, the only other known examples of Middle Jurassic microbialite-dominated structures are Bajocian to Bathonian buildups from the Bighorn Basin in northern Wyoming (Parcell and Williams, 2005; Ploynoi and Parcell, 2005). These features include thrombolite mounds (Ploynoi and Parcell, 2005), which crop out only at a single horizon along the west side of the basin, and more extensive microbial laminites (stromatolites). The stromatolites contain gypsum crystals and are associated with dinosaur footprints. These are interpreted to have been deposited in restricted marine and sabhka conditions (Parcell and Williams, 2005), differing substantially from the microbial mounds of the Amellago Canyon. The thrombolites, however, share several similarities with the Amellago mounds. All of these features are comparable in size and morphology (~1 m high and ~2–3 m wide, isolated circular mounds), composition (dense, clotted and peloidal micrite fabrics with scarce fauna), and associated facies (thrombolites above ooid grainstones overlain by highly fossiliferous sediments). The general occurrence in shallow water during periods of maximum transgression, low water energy and sediment starvation (Ploynoi and Parcell, 2005), resembles that of the Amellago mounds.

To a large extent, Bajocian sponge/microbial-crust mud-mounds of northeastern Spain, which include up to 65% microbial facies (Bersán and Aurell, 1997), share similarities with the mounds of Amellago. The Spanish mounds, although they include marked contribution from sponges, have comparable geometries (~2 m high) and internal thrombolitic fabrics. Likewise, the Spanish examples developed on top of condensed levels formed during periods of minimum sedimentation rates, and were strongly conditioned by the bathymetry, occurring only when a certain depth was reached. Bersán and Aurell (1997) speculate depths of several tens of meters, above SWWB, supported by the occurrence of reworked levels observed in the inter-mound and mound facies. This paleo-depth is slightly greater than that suggested for the studied mounds, which developed in the inner settings of the Amellago ramp, at less than 3 meters of water depth. A marked difference with the mounds of Amellago is that the ongoing development of the Spanish mounds took place during periods of high water energy when small local highs were created as sediment was redistributed. The current velocity was increased in these local highs creating a differential gradient of nutrients in these elevations and putting enough material in suspension to be baffled and bound by the sponges and microbes.

Reefs built by alternating coral and microbial crust (up to 70%) facies developed in the lower offshore to upper shoreface of a ramp setting of Bajocian strata in Haute Saône, eastern France (Olivier et al., 2006). In these examples, the microbialites encrust corals and show up to three successive growth stages (from local thin crusts of dense micrite to columnar thrombolites with clotted micrite to stromatolites that alternate with lamina of micrite/peloids with sparite). The alternating coral-microbial facies was interpreted as evidence for changing trophic resources, with periods of increased nutrient input favoring the microbialite mode. The change from a columnar thrombolite to stromatolitic was interpreted as an increase in the accumulation rate (Olivier et al., 2006). This transition in the microbialite type has been interpreted similarly in Upper Jurassic sponge-microbialite buildups (Pawallek and Aigner, 2003; Olivier et al., 2004).

The Amellago thrombolitic mounds, together with these selected Middle Jurassic examples, were limited by some common environmental conditions. During this time interval, microbialites and microbial-dominated buildups were generally scarce and only common very locally, responding to stressed environments or rapid environmental variations. On the basis of Amellago and other examples, we propose a conceptual model for the growth of fine-grained thrombolites, promoted by the combination of low sedimentation rates with changes in water depth and water energy. In this conceptual model, microbial (thrombolitic) mounds formed during transgressive stages, favored by pronounced increase in accommodation space, condensed sedimentation, and low-energy regimes. The occurrence of the thrombolite mounds only during the initial transgression within of the Assoul Formation tentatively suggests that a relative minimum depth must also be reached to favor the development of thrombolitic mounds. Such a model may serve as analogue to other Mesozoic microbial structures with similar fabrics developed in subtidal and low-energy domains of shallow carbonate platforms. In contrast, other thrombolitic examples, mainly from the Neogene, are inferred to form in areas of high water turbulence that favored non-laminar irregular accretion, physical disturbance and erosion (Braga et al., 1995).

7. Conclusions

In the Amelago Canyon of the High Atlas Mountain range of Morocco, mound structures with domal geometries are present in Bajocian carbonate strata representing inner ramp settings. These deposits consist of thrombolites with distintive homogeneous, micritic to clotted peloidal fabrics and subordinate fauna (i.e. corals, algae, bryozoans, mollusks, brachiopods and echinoids). Thrombolite fabrics formed biogenically as suggested by the pervasive clotted fabrics with even-spaced peloidal masses and by the mineralized remains of coccoid bacteria and EPS. The framboidal pyrite, observed exclusively within the thrombolitic fabric, is interpreted as a syndepositonal/early diagenetic product indicating the involvement of sulphur-reducing bacteria. The scattered displacive crystals of gypsum (now calcite pseudomorphs) precipitated during the early diagenesis from fluids generated through microbial activity.

The microbial mounds are surrounded by oolite shoals, similar to subtidal microbialites that form at present in current-swept Bahamian environments. However, the fine-grained micritic and peloidal clotted mound fabrics, virtually devoid of allochtonous coarse (fine-sand) grains, and the rounded and non-reworked mound geometries point to overall low water energy. Mound and ooid shoal developed in different environmental settings and alternated in time. During brief transitional stages, mound and shoal activity might have overlapped.

Possible controlling factors of this alternation include changes in the water energy and depth linked to low-amplitude sea-level variations. Low water energy, sub wave base conditions, substrate stability and condensed sedimentation related to transgressive stages promoted the mound formation. The limited occurrence of the microbial mounds in the onset of a trangressive event suggests that other factors, such as a certain range of water depth, a threshold in trophic conditions must be met in order to favor the growth of the microbialites. In contrast, elevated water energy during the highstand resulted in the migration of ooid shoals, which covered the mounds. The model suggested for the Amellago Bajocian microbial mounds may provide a tool to reconstruct high-frequency palaeo-environmental fluctuations and offers insight to recognize the onset of transgressive conditions that on a mesotrophic setting bring the system temporarily out of balance, into more nutrient-rich conditions, allowing widespread but short-lived microbial colonization.

Acknowledgments

The authors are grateful to G. Frijia and M. Aurell for the interesting and stimulating discussions. The critical and important comments provided by E. Rankey, M. Elrick, A. Strasser and A. Woods are acknowledged. We are also glad to thank M. Zitzmann, F. Semmo, F. Kraul and D. Bunke for their help and company in the field and C. Fischer for producing the thin-sections. Thanks to Assou, Moha and all the Agouzil family for their friendship and hospitality in the Kasbah Amellago. The ExxonMobil (FC)^2 Alliance is also thanked for generous support to this research. Comments, criticisms and suggestions from Editor B. Jones, reviewer A. Brasier and another anonymous reviewer are also much appreciated.

References

Aitken, J.D., 1967. Classification and environmental significance of cryptalgal limestones and dolomites, with illustration from the Cambrian and Ordovician of Southwestern Alberta. Journal of Sedimentary Petrology 37, 1163–1178.

Allwood, A.C., Walter, M.R., Burch, I.W., Kamber, B.S., 2007. 3.43 billion-year-old stromatolite reef from the Pilbara Craton of Western Australia: ecosystem-scale insights to early life on Earth. Precambrian Research 158, 198–227.

Aloisi, G., Gloater, A., Kruger, M., Wallmann, K., Guyot, F., Sodas, P., 2006. Nucleation of calcium carbonate on bacterial nanoglobules. Geology 34, 1017–1020.

Amour, F., Mutti, M., Christ, N., Immenhauser, A., Agar, S.M., Benson, G., Tomás, S., Alway, R., Kabiri, L., 2012. Capturing and modelling metre-scale spatial facies heterogeneity in a Jurassic ramp setting (Central High Atlas, Morocco). Sedimentology 59, 1158–1189.

Amour, F., Mutti, M., Christ, N., Immenhauser, A., Benson, G., Agar, S.M., Tomás, S., Kabiri, L., 2013. Outcrop analog for an oolitic carbonate ramp reservoir: a scale-dependent geological modeling approach based on stratigraphic hierarchy. AAPG Bulletin 97, 845–871.

Andres, M.S., Reid, R.P., 2006. Growth morphologies of modern marine stromatolites: a case study from Highborne Cay, Bahamas. Sedimentary Geology 185, 319–328.

Arp, G., Reimer, A., Reitner, J., 2001. Photosynthesis-induced biofilm calcification and calcium concentrations in Phanerozoic oceans. Science 292, 1701–1704.

Beauchamp, W., Allmendinger, R.W., Barazangi, M., 1996. Inversion tectonics and the evolution of the High Atlas Mountains, Morocco, based on a geological-geophysical transect. Tectonics 18, 163–184.

Bersán, R., Aurell, M., 1997. Origen y desarrollo de los montículos de esponjas y algas del Bajociense superior de Ricla (Cordillera Ibérica Septentrional). Cuadernos de Geologia Iberica 22, 65–80.

Braga, J.C., Martin, J.M., Riding, R., 1995. Controls on microbial dome fabric development along a carbonate-silicicastic shelf-basin transect, Miocene, SE Spain. Palaios 10, 347–361.

Brede, R., Hauptmann, M., Herbig, H., 1992. Plate tectonics and intracratonic mountain ranges in Morocco: the Mesozoic–Cenozoic development of the central High Atlas and the Middle Atlas. Geologische Rundschau 81, 127–141.

Burchette, T.P., Wright, V.P., 1992. Carbonate ramp depositional systems. Sedimentary Geology 79, 3–57.

Burgess, P.M., 2008. The nature of shallow-water carbonate lithofacies thickness distribution. Geology 36, 235–238.

Burne, R.V., Moore, L.S., 1987. Microbialites: organosedimentary deposits of benthic microbial communities. Palaios 2, 241–254.

Burns, B.P., Anitori, R., Butterworth, P., Henneberger, R., Goh, F., Allen, M.A., Ibanez-Peral, R., Bergquist, P.L., Walter, M.R., Neilan, A., 2009. Modern analogues and the early history of microbial life. Precambrian Research 1–38.

Byrne, M., Morris, P., Wentworth, S., Thomas-Keprta, K., Brigmon, R., McKay, D., 2001. Biogenic structures from a hypersaline lake in the Bahamas. Lunar and Planetary Science XXXII, Houston, Texas. (abstract no. 1068).

Camoin, G.F., Cabioch, G., Eisenhauer, A., Braga, J.C., Hamelin, B., Lericolais, G., 2006. Environmental significance of microbialites in reef environments during the last deglaciation. Sedimentary Geology 185, 277–295.

Cayeux, M., 1935. Les Roches Sédimentaires de France. Roches Carbonatées. Masson, Paris (463 pp.).

Chafetz, H.S., 1986. Marine peloids; a product of bacterially induced precipitation of calcite. Journal of Sedimentary Petrology 56, 812–817.

Christ, N., Immenhauser, A., Amour, F., Mutti, M., Tomás, S., Agar, S.M., Alway, R., Kabiri, L., 2012. Characterization and interpretation of discontinuity surfaces in a Jurassic ramp setting (High Atlas, Morocco). Sedimentology 59, 249–290.

Défarge, C., Trichet, J., Jaunet, A.M., Robert, M., Tribble, J., Sansone, F.J., 1996. Texture of microbial sediments revealed by cryo-scanning electron microscopy. Journal of Sedimentary Research 66, 935–947.

Dill, R.F., 1991. Subtidal stromatolites, ooids, and crusted-lime muds at Great Bahama Bank margin. In: Osborne, R.H. (Ed.), From Shoreline to Abyss: Contributions in marine geology in honour of Francis Parker ShephardSEPM Special Publication 46, 147–171.

Dill, R.F., Shinn, E., Jones, A., Kelly, K., Steinen, R., 1986. Giant subtidal stromatolites forming in normal salinity waters. Nature 324, 55–58.

Dravis, J.J., 1983. Hardened subtidal stromatolites, Bahamas. Science 219, 385–386.

Dromart, G., 1992. Jurassic deep-water microbial biostromes flooding markers in carbonate sequence stratigraphy. Palaeogeography, Palaeoclimatology, Palaeoecology 91, 219–228.

Dupraz, C., Strasser, A., 1999. Microbialites and micro-encrusters in shallow coral bioherms (Middle to Late Oxfordian, Swiss Jura Mountains). Facies 40, 101–130.

Dupraz, C., Visscher, P.T., Baumgartner, L., Reid, R.P., 2004. Microbe-mineral interactions: early carbonate precipitation in a hypersaline lake (Eleuthera Island, Bahamas). Sedimentology 51, 745–765.

Dupraz, C., Reid, R.P., Braissant, O., Decho, A.W., Norman, R.S., Visscher, P.T., 2009. Processes of carbonate precipitation in modern microbial mats. Earth-Science Reviews 96, 141–162.

Feldmann, M., McKenzie, J.A., 1998. Stromatolite - thrombolite associations in a modern environment, Lee Stocking Island, Bahamas. Palaios 13, 201–212.

Fischer, A.G., 1965. Fossils, early life, and atmospheric history. Proceedings of the National Academy of Science USA, 53. National Academy of Sciences, Washington, pp. 1205–1215.

Friebe, A., 1995. Die Schwammfazies im Mitteljura des nordöstlichen Keltiberikums (Spanien). Profil 8, 239–279.

Ginsburg, R.N., Planavski, N.J., 2008. Diversity of Bahamian Microbialite Substrates. In: Dilek, Y., Furnes, H., Muehlenbachs, K. (Eds.), Links between geological processes, microbial activities & evolution of life: Modern Approaches in Solid Earth Sciences, 4, pp. 177–195.

Grotzinger, J.P., 1990. Geochemical model for Proterozoic stromatolite decline. American Journal of Science 290-A, 80–103.

Grotzinger, J.P., Knoll, A.H., 1999. Stromatolites in Precambrian carbonates: evolutionary mileposts or environmental dipsticks? Annual Reviews of Earth and Planetary Sciences 27, 313–358.

Hallock, P., Schlager, W., 1986. Nutrient excess and the demise of coral reefs and carbonate platforms. Palaios 1, 389–398.

Harwood, C.L., Summer, D.Y., 2011. Microbialites of the Neoproterozoic Beck Spring Dolomite, Southern California. Sedimentology 58, 1648–1673.

Hofmann, H.J., Grey, A.H., Hickman, A.H., Thorpe, R.I., 1999. Origin of 3.45 Ga coniform stromatolites in Warrawoona Group, Western Australia. Geological Society of America Bulletin 111, 1256–1262.

Immenhauser, A., Hillgärtner, H., Van Bentum, E., 2005. Microbial-foraminiferal episodes in the Early Aptian of the southern Tethyan margin: Ecological significance and possible relation to oceanic anoxic event 1a. Sedimentology 52, 77–99.

Jacobshagen, V., Brede, R., Hauptmann, M., Heinitz, W., Zylka, R., 1988. Structure and post-Palaeozoic evolution of the central High Atlas. In: Jacobshagen, V. (Ed.), The Atlas System of Morocco: Lecture Notes in Earth Science, 15, pp. 245–271.

Jahnert, R., Collins, L., 2013. Controls on microbial activity and tidal flat evolution in Shark Bay, Western Australia. Sedimentology. http://dx.doi.org/10.1111/sed.12023.

Kazmierczak, J., Coleman, M., Gruszczynski, M., Kempe, S., 1996. Cyanobacterial key to the genesis of micritic and peloidal limestones in ancient seas. Acta Palaeontologka Polonica 41, 319–338.

Kazmierczak, J., Altermann, W., Kremer, B., Kempe, S., Eriksson, P., 2009. Mass occurrence of benthic coccoid cyanobacteria and their role in the production of Neoarchean carbonates of South Africa. Precambrian Research 173, 79–92.

Kempe, S., Kazmierczak, J., Landmann, G., Konuk, T., Reimer, A., Lipp, A., 1991. Largest known microbialites discovered in Lake Van, Turkey. Nature 349, 605–608.

Kennard, J., James, N., 1986. Thrombolites and stromatolites: two distinct types of microbial structures. Palaios 1, 492–503.

Keupp, H., Jenisch, A., Herrmann, R., Neuweiler, F., Reitner, J., 1993. Microbial carbonate crusts — a key to the environmental analysis of fossil spongiolites? Facies 29, 41–54.

Laville, E., Pique, A., Amrahr, M., Charroud, M., 2004. A restatement of the Mesozoic Atlasic Rifting (Morocco). Journal of African Earth Science 38, 145–153.

Leinfelder, R.R., 1993. Upper Jurassic reef types and controlling factors — a preliminary report. Profil 5, 1–45.

Leinfelder, R.R., Schmid, D.U., 2000. Mesozoic reefal thrombolites and other microbolites. In: Riding, R., Awramik, S.M. (Eds.), Microbial Sediments. Springer, Berlin, pp. 289–294.

Leinfelder, R.R., Nose, M., Schmid, D.U., Werner, W., 1993. Microbial crusts of the Late Jurassic: composition, palaeoecological significance and importance in reef construction. Facies 29, 195–230.

Leinfelder, R.R., Werner, W., Nose, M., Schmid, D.U., Krautter, M., Laternser, R., Takacs, M., Hartmann, D., 1996. Paleoecology, growth parameters and dynamics of coral, sponge and microbolite reefs from the Late Jurassic. In: Reitner, J., Neuweiler, F., Gunkel, F. (Eds.), Global and regional controls on biogenic sedimentation, I, Reef Evolution, Research Reports: Göttinger Arbeiten zur Geologie und Paläontologie, 2, pp. 227–248.

Logan, B.W., 1961. Cryptozoon and associated stromatolites from the Recent, Shark Bay, Western Australia. Journal of Geology 69, 517–533.

Macintyre, I.G., 1985. Submarine cements — the peloidal question. In: Schneidermann, N., Harris, P.M. (Eds.), Carbonate CementsSEPM Special Publication 36, 109–116.

McCook, L.J., 2001. Competition between corals and algal turfs along a gradient of terrestrial influence in the nearshore central Great Barrier Reef. Coral Reefs 19, 419–425.

McKee, E.D., Gutschick, R.C., 1969. Analysis of lithology. In: McKee, E.D., Gutschick, R.C. (Eds.), History of the Redwall Limestone of Northern ArizonaGeological Society of America, Memoirs 114, 97–124.

Monty, C.L.V., 1976. The origin and development of cryptalgal fabrics. In: Walter, M.R. (Ed.), Stromatolites. Developments in Sedimentology, 20. Elsevier, Amsterdam, pp. 193–249.

Mutti, M., Hallock, P., 2003. Carbonate systems along nutrient and temperature gradients: some sedimentological and geochemical constraints. International Journal of Earth Sciences 92, 465–475.

Olivier, N., Pittet, B., Mattioli, E., 2004. Paleoenvironmental control on sponge-reefs and contemporaneous deep-shelf-marl-limestone deposition (Late Oxfordian, southern Germany). Palaeogeography, Palaeoclimatology, Palaeoecology 212, 233–263.

Olivier, N., Lathuilière, B., Thiry-Bastien, P., 2006. Growth models of Bajocian coral-microbialite reefs of Chargey-lès-Port (eastern France): Palaeoenvironmental interpretations. Facies 52, 113–127.

Paerl, H.W., Steppe, T.F., Reid, R.P., 2001. Bacterially mediated precipitation in marine stromatolites. Environmental Microbiology 3, 123–130.

Parcell, W.C., Williams, M.K., 2005. Mixed sediment deposition in a retro-arc foreland basin: Lower Ellis Group (M. Jurassic), Wyoming and Montana, U.S.A. Sedimentary Geology 177, 175–194.

Pawallek, T., Aigner, T., 2003. Apparently homogenous “reefs”-limestones built by high-frequency cycles: Upper Jurassic, SW-Germany. Sedimentary Geology 160, 259–284.

Pedley, M., 2013. The morphology and function of thrombolitic calcite precipitating biofilms: a universal model derived from freshwater mesocosm experiments. Sedimentology. http://dx.doi.org/10.1111/sed.12042.

Pierre, A., Durlet, C., Razin, P., Chellai, E.H., 2010. Spatial and temporal distribution of ooids along a Jurassic carbonate ramp: Amellago transect, High Atlas, Morocco. Geological Society of London, Special Publication 329, 65–88.

Planavsky, N., Ginsburg, R.N., 2009. Taphonomy of modern marine Bahamian microbialites. Palaios 24, 5–17.

Ploynoi, M., Parcell, W.C., 2005. Development of Middle Jurassic microbial buildups in Bighorn Basin, Wyoming. Geological Society of America Annual Meeting Abstracts with Programs 37, 17.

Pratt, B.R., 1995. The origin, biota and evolution of deep-water mud-mounds. In: Monty, C.L.V., Bosence, D.W.J., Bridges, P.H., Pratt, B.R. (Eds.), Carbonate Mud-Mounds, Their Origin and Evolution. Special Publication, 23. International Association of Sedimentologists, pp. 49–123.

Rameil, N., Immenhauser, A., Warrlich, G., Hillgärtner, H., Droste, H.J., 2010. Morphological patterns of Aptian *Lithocodium–Bacinella* geobodies: relation to environment and scale. Sedimentology 57, 883–911.

Reid, R.P., Macyntire, I.G., Browne, K.M., Steneck, R.S., Miller, T., 1995. Modern marine stromatolites in the Exuma Cays, Bahamas: uncommonly common. Facies 33, 1–18.

Reid, R.P., Visscher, P.T., Decho, A.W., Stolz, J.F., Bebout, B.M., Dupraz, C., Macintyre, I.G., Paerl, H.W., Pinckney, J.L., Prufert-Bebout, L., Steppe, T.F., DesMarais, D.J., 2000. The role of microbes in accretion, lamination and early lithification of modern marine stromatolites. Nature 406, 989–992.

Reid, R.P., James, N.P., Macyntire, I.G., Dupraz, C., Burne, R.V., 2003. Shark bay stromatolites: microfabrics and reinterpretations of origins. Facies 49, 45–53.

Reolid, M., Molina, J.M., Löser, H., Navarro, V., Ruiz-Ortiz, P.A., 2009. Coral biostromes of the Middle Jurassic from the Subbetic (Betic Cordillera, southern Spain): facies, coral taxonomy, taphonomy, and paleoecology. Facies 55, 575–593.

Riding, R., 1991. Classification of microbial carbonates. In: Riding, R. (Ed.), Calcareous Algae and Stromatolites. Springer, Berlin, pp. 22–51.

Riding, R., 1992. Temporal variation in calcification in marine cyanobacteria. Journal of the Geological Society of London 149, 979–989.

Riding, R., 2000. Microbial carbonates: the geological record of calcified bacterial–algal mats and biofilms. Sedimentology 47, 179–214.

Riding, R., 2002. Biofilm architecture of Phanerozoic cryptic carbonate marine veneers. Geology 30, 31–34.

Riding, R., 2006. Cyanobacterial calcification, carbon dioxide concentrating mechanisms, and Proterozoic–Cambrian changes in atmospheric composition. Geobiology 4, 299–316.

Riding, R., 2008. Abiogenic, microbial and hybrid authigenic carbonate crusts: components of Precambrian stromatolites. Geologia Croatica 61, 73–103.

Riding, R., 2011. Microbialite, stromatolites, and thrombolites. In: Reitner, V., Thiel, J. (Eds.), Encyclopedia of Geobiology (Encyclopedia of Earth Sciences Series). Springer, Heidelberg, pp. 635–654.

Riding, R., Liang, L., 2005. Geobiology of microbial carbonates: metazoan and seawater saturation state influences on secular trends during the Phanerozoic. Palaeogeography, Palaeoclimatology, Palaeoecology 219, 101–115.

Riding, R., Tomás, S., 2006. Stromatolite reef crusts, Early Cretaceous, Spain: Bacterial origin of *in situ*-precipitated peloid microspar? Sedimentology 53, 23–34.

Riding, R., Braga, J.C., Martín, J.M., 1991. Oolite stromatolites and thrombolites, Miocene, Spain: analogues of Recent giant Bahamian examples. Sedimentary Geology 71, 121–127.

Shapiro, R.S., 2000. A comment on the systematic confusion of thrombolites. Palaios 15, 166–169.

Spadafora, A., Perri, E., McKenzie, J., Vasconcelos, C., 2010. Microbial biomineralization processes forming modern Ca: Mg carbonate stromatolites. Sedimentology 57, 27–40.

Strasser, A., 1986. Ooids in Purbeck limestones (Lowermost Cretaceous) of the Swiss and French Jura. Sedimentology 33, 711–727.

Strasser, A., Pittet, B., Hillgärtner, H., Pasquier, J.B., 1999. Depositional sequences in shallow carbonate-dominated sedimentary system: concepts of high-resolution analysis. Sedimentary Geology 128, 201–221.

Sun, S.Q., Wright, V.P., 1989. Peloidal fabrics in Upper Jurassic reefal limestones, Weald Basin, southern England. Sedimentary Geology 65, 165–181.

Wilmsen, M., Neuweiler, F., 2008. Biosedimentology of the Early Jurassic post-extinction carbonate depositional system, central High Atlas rift basin, Morocco. Sedimentology 55, 773–807.